CHEMISTRY
A EUROPEAN JOURNAL

DOI: 10.1002/chem.200802206

Photoinduced Reactions of *cis*,*trans*,*cis*-[$Pt^{IV}(N_3)_2(OH)_2(NH_3)_2$] with 1-Methylimidazole

Hazel I. A. Phillips,[a] Luca Ronconi,[b, c] and Peter J. Sadler*[a]

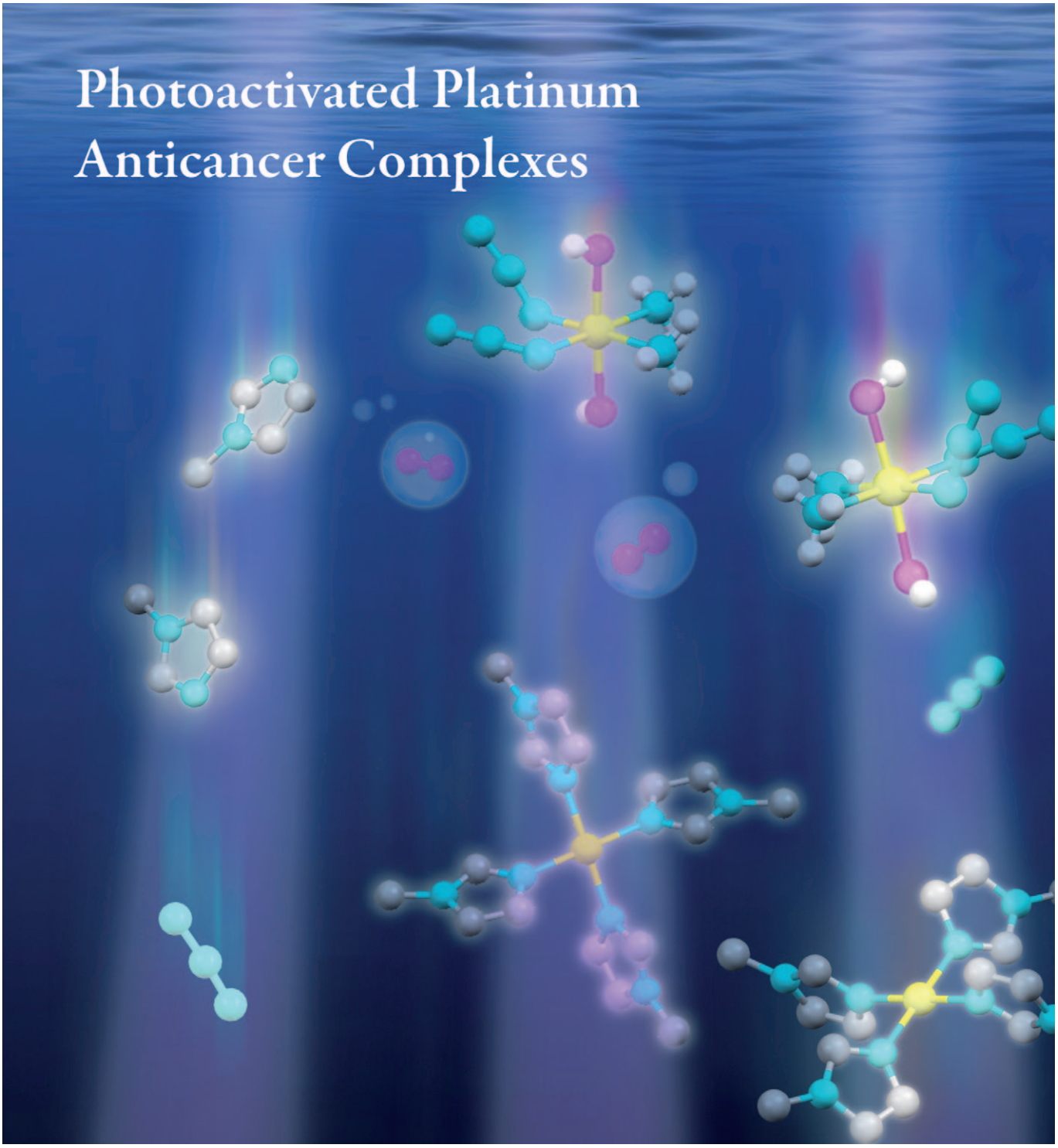

Abstract: The photodecomposition of *cis*,*trans*,*cis*-$[Pt^{IV}(N_3)_2(OH)_2(NH_3)_2]$ in phosphate buffered saline (PBS), as well as in the presence of 1-methylimidazole (1-MeIm), induced by UVA light (centred at $\lambda = 365$ nm) has been studied by multinuclear NMR spectroscopy. We show that photoreduction, photoisomerisation and *trans*-labilisation pathways are involved. The photodecomposition pathway in PBS, which involves azide release, as detected by ^{14}N NMR spectroscopy, appears to differ from that in acidic aqueous conditions, under which N_2 is a product. A number of *trans*-{N-Pt^{II}-NH_3} species were also observed as photoproducts, as well as the release of free ammonia with a corresponding increase in pH. Oxygen was also detected as a product in solution. In the presence of 1-methylimidazole, surprisingly the major photoproduct was the tetra-substituted Pt^{II} complex $[Pt^{II}(1\text{-MeIm-}N^3)_4]^{2+}$ (structure confirmed by crystallography), even at a Pt/1-MeIm molar ratio of 1:1, together with *cis*- and *trans*-$[Pt^{II}(NH_3)_2(1\text{-MeIm-}N^3)_2]^{2+}$ as minor products. In these photoinduced 1-MeIm reactions, free ammonia, azide and oxygen were also detected. The results from this study illustrate that photoinduced reactions of platinum complexes can lead to novel reaction pathways, and therefore to new cytotoxic mechanisms in cancer cells.

Keywords: azides · bioinorganic chemistry · drug discovery · NMR spectroscopy · photochemistry · platinum

Introduction

Photoactivation provides an interesting mechanism for reduction of Pt^{IV} to Pt^{II}. Pt^{IV} complexes can be made photolabile by choosing appropriate ligands, for example, Pt^{IV}–azido complexes are known to be photoactive.[1,2] Such platinum complexes can then undergo a variety of photochemical reactions, including isomerisation, substitution and reduction. A possible application of such processes is for therapeutic purposes and the development of light-sensitive Pt^{IV} pro-drugs that can be photoactivated (e.g. with laser light) to active antitumour agents directly at the site of the tumour.[3,4] Such site-selective activation would be expected to lead to a decrease in side-effects and toxicity, and an increase in the therapeutic index. Hence, the clinical usefulness of platinum antitumour agents might be expanded. Therefore, we have developed a series of complexes of the form $[Pt^{IV}(N_3)_2(OH)_2(amine)_2]$, such as *cis*,*trans*,*cis*-$[Pt^{IV}(N_3)_2(OH)_2(NH_3)_2]$ (**1**), which exhibit little or no dark toxicity, but bind to DNA upon photoactivation.[3,4]

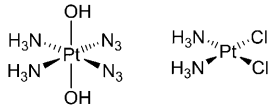

1 **2**

Transcription mapping studies with treated plasmid DNA have shown that the platination sites resemble those from reaction with cisplatin (**2**) in dark conditions.[5] However, these complexes appear to kill cancer cells through a mechanism different from those of the classical platinum-based drugs.[6,7] In the photoreduction of Pt^{IV}–diazido precursors to their Pt^{II} counterparts, a possible mechanism involves the release of azido ligands as $N_3^{\cdot}$ radicals. Azidyl radicals are very unstable and rapidly decompose in water into molecular nitrogen (N_2), thus preventing reoxidation of the platinum centre (Scheme 1).[8]

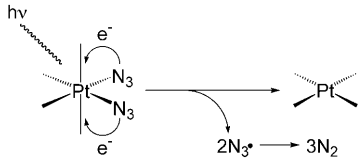

Scheme 1. Possible mechanism for the photoreduction of Pt^{IV}-diazido complexes.

We report here studies of the photodecomposition pathways in phosphate buffered saline (PBS) solution of complex **1** both on its own and in the presence of the nitrogen heterocycle 1-methylimidazole (1-MeIm). Imidazole fragments are an important part of purines, such as guanosine, xanthine, theophylline, 8-methylcaffeine, and histidyl residues in proteins. For example, in the enzyme carbonic anhydrase, the active site involves coordination of Zn^{II} to the imidazole ring nitrogen atom of histidine,[9] and in the serine proteases, the pH-dependent protonation–deprotonation of the imidazole ring of histidine plays an important role in the mechanism of peptide bond cleavage.[10] In addition to inter- and intrastrand cross-links with DNA (involving especially binding to N^7 of guanine bases), Pt^{II} complexes also form DNA–protein cross-links involving histidine-, cysteine- and methionine-rich proteins.[11–13] Thus, 1-methylimidazole is a

[a] H. I. A. Phillips, P. J. Sadler
Department of Chemistry
University of Warwick
Gibbet Hill Road, Coventry CV4 7AL (UK)
Fax: (+44) 24-7652-3819
E-mail: P.J.Sadler@warwick.ac.uk

[b] L. Ronconi
School of Chemistry
University of Edinburgh
West Mains Road, Edinburgh EH9 3 JJ (UK)

[c] L. Ronconi
Current address: Department of Chemical Sciences
University of Padova, Via Marzolo 1, Padova 35131 (Italy)

Supporting information for this article is available on the WWW under http://dx.doi.org/10.1002/chem.200802206.

useful model for studies of photoinduced reactions of these Pt^{IV}-diazido complexes.

In particular, we have used here multinuclear NMR methods, including ^{14}N NMR spectroscopy, to track photoreaction pathways involving the azido ligands. The elucidation of such photochemical pathways aids the understanding of the biological mechanism of action for this group of complexes.

Results

Photochemical behaviour of complex 1 in PBS solution: First, we recorded a 1D $^{14}N\{^1H\}$ NMR spectrum of the unlabelled complex **1** in PBS solution in dark conditions (Figure 1a). Peaks **a** (353.3), **b** (227.4) and **c** (160.5 ppm) are assigned to the terminal, central and Pt^{IV}-bound nitrogen atoms, respectively, of the coordinated azido ligands. The upfield peak **d** at −40.8 ppm ($^1J(^{195}Pt\text{-}^{14}N) = 180$ Hz) is consistent with an ammine ligand bound to a Pt^{IV} metal centre *trans* to a nitrogen donor ligand.[14] Upon irradiation of the sample with UVA light for 10 min ($\lambda_{max} = 365$ nm, P = 7.3 mW cm^{-2} (P = power level), dose = 4.4 J cm^{-2}) at 310 K, new ^{14}N signals appeared (Figure 1b). Peaks **a** (353.4), **b** (227.5) and **c** (161.1 ppm) for the azido ligands of **1** were still present, but with reduced intensities, and the new peaks **a′** (76.9) and **b′** (225.7 ppm) appeared, which are assignable to the terminal and central nitrogen atoms of free azide

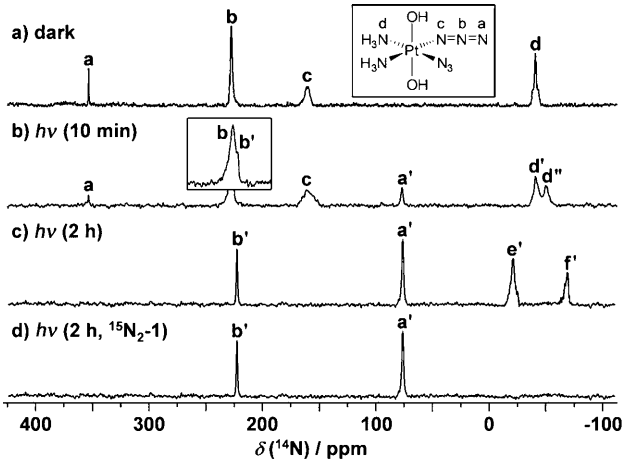

Figure 1. 1D $^{14}N\{^1H\}$ NMR spectra of complex **1** (12.6 mM in 90% PBS/10% D_2O, Ar-saturated, initial pH 7.4) a) in the dark, b) after 10 min of irradiation ($\lambda_{max} = 365$ nm, P = 7.3 mW cm^{-2}, dose = 4.4 J cm^{-2}) at 310 K, c) after 2 h of irradiation ($\lambda_{max} = 365$ nm, P = 7.3 mW cm^{-2}, dose = 56.6 J cm^{-2}, final pH 10.1) at 310 K. d) 1D $^{14}N\{^1H\}$ NMR spectrum of complex $^{15}N_2$-**1** (14.8 mM in 90% H_2O/10% D_2O, Ar-saturated, initial pH 7.4) after 2 h of irradiation ($\lambda_{max} = 365$ nm, P = 7.2 mW cm^{-2}, dose = 52.0 J cm^{-2}, final pH 9.9) at 310 K. Assignments: **a**, **b**, **c**, coordinated azido ligand ($\delta = 353.3$ (Pt^{IV}-NN***N***), 227.4 (Pt^{IV}-N***N***N), 160.5 ppm (Pt^{IV}-***N***NN)) as labelled in structure; **a′**, **b′**, free azide (N_3^-; $\delta = 76.9$ (***N***N***N***), 225.7 ppm (N***N***N)); **d**, chemical shift consistent with *t*-{N-Pt^{IV}-NH_3} species ($\delta = -40.8$ ppm); **d′**, **d″**, chemical shifts consistent with *t*-{N/O-Pt^{IV}-NH_3} species ($\delta = -40.9$ ppm, −50.8 ppm); **e′**, free ammonia (NH_3; $\delta = -20.9$ ppm); **f′**, chemical shift consistent with *t*-{N/O-Pt^{II}-NH_3} species ($\delta = -69.6$ ppm).

(N_3^-) in solution, in accordance with literature data.[15] New peaks **d′** (−40.9) and **d″** (−50.8 ppm) are assignable to ammine groups coordinated to a Pt^{IV} centre *trans* to nitrogen and oxygen donor ligands, respectively.[14] Intriguingly, no peaks for either N_2 (sharp peak expected at ca. 287 ppm[15]) or for Pt^{II}–NH_3 species (expected in the range −60 to −90 ppm)[14] were observed. Remarkably, similar results were obtained upon irradiation at 310 K with either UVA light for 2 h at a much lower power ($\lambda_{max} = 365$ nm, P = 0.6 mW cm^{-2}, dose = 4.5 J cm^{-2}), or with UV-Visible light ($\lambda = 250$-700 nm) for 6 h (P = 30.0 mW cm^{-2}, dose = 648.0 J cm^{-2}; data not shown).

When UVA irradiation was prolonged for 2 h, the final pH of the solution increased to 10.1 (despite the initial attempt to buffer the solution with 10 mM phosphate), and no ^{14}N peaks assignable to either coordinated azides or N_2 were detected. The two new sharp signals at 77.0 (**a′**) and 225.6 ppm (**b′**; Figure 1c) are due to the terminal and central nitrogen atoms, respectively, of free N_3^- in solution, whereas the chemical shift of peak **f′** (−69.6 ppm) is consistent with an Pt^{II}–NH_3 fragment *trans* to N- and/or O-donor ligands (broad, perhaps due to overlapping peaks).[14] Finally, new peak **e′** (−20.9 ppm) is due to the presence of free ammonia in solution, consistent with the increase of pH upon irradiation. Some precipitate formed during the photoreaction and is likely to arise from polymeric hydroxo-/oxo-bridged Pt species, which arise partly as a result of ammonia release, hydrolysis and deprotonation of aqua/hydroxo ligands.[16]

A similar experiment was carried out using the $^{15}NH_3$-labelled analogue of complex **1** ($^{15}N_2$-**1**). The 1D $^{14}N\{^1H\}$ NMR spectrum of $^{15}N_2$-**1** (14.8 mM in 90% PBS/10% D_2O, Ar-saturated, initial pH 7.4) obtained after 2 h of irradiation ($\lambda_{max} = 365$ nm, P = 7.2 mW cm^{-2}, dose = 52.0 J cm^{-2}) at 310 K is shown in Figure 1d. Again, the pH increased (to 9.9), insoluble precipitate formed during the photoreaction and the two new peaks (**a′** and **b′**) due to free azide in solution were detected. As expected, no ^{14}N NMR signals assignable to Pt–NH_3 moieties were detected, as the coordinated ammine groups were ^{15}N-labelled. After performing ^{14}N NMR experiments, the pH of the solution was re-adjusted to 3.1 with dilute $HClO_4$ to ensure slow exchange of NH protons, and 1D ^1H and 2D [^1H,^{15}N] HSQC NMR experiments were carried out. Only one major Pt^{II}–ammine species was detected at $\delta(^1H/^{15}N) = 4.05/-68.7$ ppm ($^1J(^{15}N\text{-}H) = 72$ Hz, $^1J(^{195}Pt,^{15}N) = 282$ Hz, $^2J(^{195}Pt,H) = 56$ Hz), which is consistent with a *trans*-{$Pt^{II}(NH_3)_2$} fragment.[17,18] This suggests that photoisomerisation can accompany the main photoreduction process, and no other Pt^{II} or Pt^{IV} species were observed. In addition, a new peak at $\delta(^1H/^{15}N) = 7.12/-1.90$ ppm was detected, assignable to free $^{15}NH_4^+$ in solution, which is consistent with the release of some ^{15}N-labelled ammine ligands upon irradiation. The possible formation of Pt–phosphate adducts was ruled out by performing 1D $^{31}P\{^1H\}$ NMR experiments, in which only one ^{31}P signal was observed at 1.2 ppm due to the free buffer itself. Remarkably, very similar results were obtained when the photoreactions were carried out in phosphate buffer in the ab-

sence of Cl^- ions, thus ruling out the formation of Pt–chlorido derivatives and the possible role of chlorides in the photoredox process (data not shown).

Evolution of oxygen upon UVA irradiation of complex 1: To explore other potential photoreduction pathways, we investigated the possible evolution of gaseous dioxygen after irradiation by means of a Po_2 electrode. A 10.56 mM solution of complex **1** in PBS solution (initial pH 7.4) was Ar-saturated for 30 min and irradiated for 2 h ($\lambda_{max}=365$ nm, $P=6.3\ mW\,cm^{-2}$, dose $=45.6\ J\,cm^{-2}$) at 310 K. After irradiation, the pH increased to 10.0 and a Po_2 value of 64 mmHg was recorded.

Photochemical behaviour of complex 1 in PBS solution in presence of 1-methylimidazole: First we studied the pH dependence of the ^{14}N NMR shifts of 1-methylimidazole (1-MeIm). The imidazole ring is a particularly important constituent of biological systems (e.g., a histidyl side chain in proteins) primarily because of its acid–base equilibrium with a unique pK_a value (7.1) near to neutrality in aqueous solution.[19] This gives the imidazole ring the capability, in many biological fluids, of acting as a proton donor or acceptor and, perhaps most importantly, as a ligand which can coordinate to metal ions.

^{14}N NMR shifts for N^1 and N^3 of 1-methylimidazole in aqueous solution as a function of pH are plotted in Figure 2a. As expected, protonation of 1-methylimidazole at N^3 produces a large shift of the N^3 resonance (ca. 71 ppm upfield) and a comparatively small shift of N^1 resonance (ca. 7 ppm downfield) relative to the deprotonated species. The pK_a of 7.15 ± 0.06 is in good agreement with the reported value of 7.2.[19] At low pH, $^{14}N^1$ and $^{14}N^3$ resonances essentially superimpose, as well as the ^1H NMR peaks of H^4 and H^5 protons (Figure 2b), in agreement with reported data.[19]

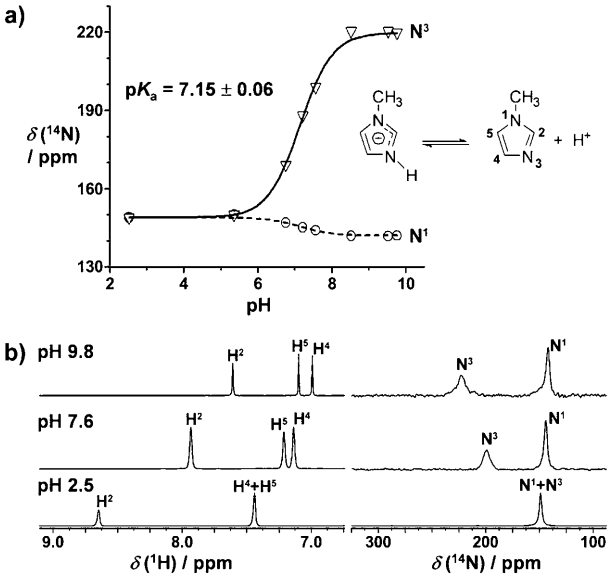

Figure 2. a) pH dependence of ^{14}N NMR shifts of N^1 and N^3 of 1-methylimidazole. The pK_a value was determined as described in the Experimental Section. b) Representative 1D ^1H and $^{14}N\{^1H\}$ NMR spectra of 1-methylimidazole (62.7 mM in 90% H_2O/10% D_2O) at pH 2.5, 7.6 and 9.8.

The interaction between the ^{15}N-labelled analogue of complex **1** ($^{15}N_2$-**1**) and 1-methylimidazole in PBS solution was investigated. An 8.6 mM solution of $^{15}N_2$-**1** in 90% PBS/10% D_2O was prepared and 1-methylimidazole added (molar ratio = 1:1.02) at a starting pH of 8.7 (no adjustment). After degassing the solution with Ar for 30 min, the sample was irradiated for 2 h ($\lambda_{max}=365$ nm, $P=6.4\ mW\,cm^{-2}$, dose $=46.1\ J\,cm^{-2}$) at 310 K, and the photoproducts were characterised by NMR spectroscopy. The solution, initially pale yellow, turned colourless after irradiation, and no precipitate formed. As already observed after irradiating complex $^{15}N_2$-**1** on its own, the pH increased to 10.2. In the 1D $^{14}N\{^1H\}$ NMR spectrum, several signals were detected. The two new sharp signals at 77.0 (**a′**) and 225.7 ppm (**b′**; Figure 3) are due to the terminal and central

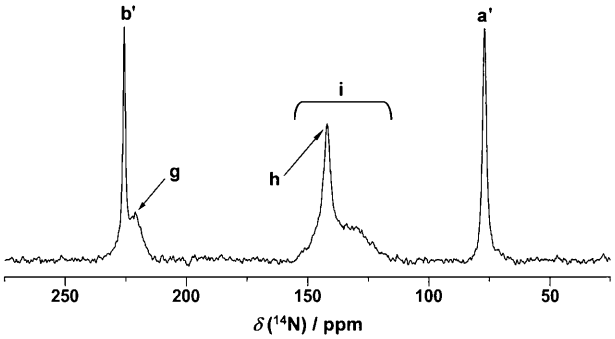

Figure 3. 1D $^{14}N\{^1H\}$ NMR spectrum of complex $^{15}N_2$-**1** (8.6 mM) in presence of 1-methylimidazole (molar ratio 1:1.02) in 90% PBS/10% D_2O (Ar-saturated, initial pH 8.7) after 2 h of irradiation ($\lambda_{max}=365$ nm, $P=6.4\ mW\,cm^{-2}$, dose $=46.1\ J\,cm^{-2}$, final pH 10.2) at 310 K. Assignments: **a′**, **b′**, free azide (N_3^-) in solution ($\delta=77.0$ (***N*N*N***,), 225.7 ppm (N***N*N***,)); **g** (***N*^3^***), **h** (***N*^1^***), free 1-methylimidazole in solution ($\delta=221.1$, 141.9 ppm); **i**, broad signal indicating N^3 and N^1 atoms of Pt-coordinated 1-methylimidazole ($\delta=150$-123 ppm).

nitrogen atoms of free N_3^- in solution, respectively, whereas new peaks **g** (221.1) and **h** (141.9 ppm) are assigned to the N^3 and N^1 atoms of free 1-methylimidazole. The new broad signal **i** in the range 150–123 ppm is assignable to the N^3 and N^1 atoms of Pt-coordinated 1-methylimidazole. As previously observed, no peaks assignable to either coordinated azides or N_2 were detected. In contrast, evolution of gaseous dioxygen was again detected potentiometrically soon after irradiation, giving a Po_2 value of 50 mmHg.

Six different 1-methylimidazole-containing species were detected with the aid of 1D ^1H (Figure 4), 2D [^1H,^1H] NOESY (Figure 5), [^1H,^{13}C] HSQC, and [^1H,^{15}N] HMBC (Figure 6) NMR spectroscopy. Their chemical shifts are summarised in Table 1. The major species (γ) can be identified as $[Pt^{II}(1\text{-MeIm-}N^3)_4]^{2+}$, supported by the X-ray structure of crystals obtained under similar experimental conditions (see Supporting Information). The crystal structure of this complex has been reported previously by Clement and co-workers (CCDC ref. code: HIGVUO01).[20] The presence of ClO_4^- as the counterion arises from the use of perchloric acid for pH adjustment. This square-planar complex con-

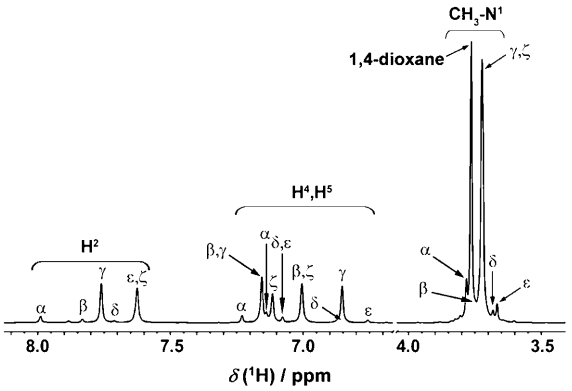

Figure 4. 1D ^{1}H NMR spectrum of complex $^{15}N_2$-**1** (8.6 mM) in presence of 1-methylimidazole (molar ratio 1:1.02) in 90% PBS/10% D_2O (Ar-saturated, initial pH 8.7) after 2 h of irradiation (λ_{max} = 365 nm, P = 6.4 mW cm^{-2}, dose = 46.1 J cm^{-2}, final pH 10.2) at 310 K. α = *trans*-[Pt^{II}(NH$_3$)$_2$(1-MeIm-N^3)$_2$]$^{2+}$; β = *cis*-[Pt^{II}(NH$_3$)$_2$(1-MeIm-N^3)$_2$]$^{2+}$; γ = [Pt^{II}(1-MeIm-N^3)$_4$]$^{2+}$; δ,ε = unidentified, ζ = free 1-MeIm. See Table 1 for species assignment.

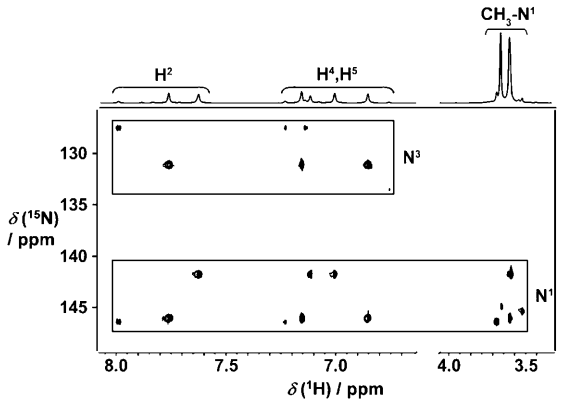

Figure 6. 2D [^{1}H, ^{15}N] HMBC NMR spectrum of complex $^{15}N_2$-**1** (8.6 mM) in presence of 1-methylimidazole (molar ratio 1:1.02) in 90% PBS/10% D_2O (Ar-saturated, initial pH 8.7) after 2 h of irradiation (λ_{max} = 365 nm, P = 6.4 mW cm^{-2}, dose = 46.1 J cm^{-2}, final pH 10.2) at 310 K. See Table 1 for species assignment.

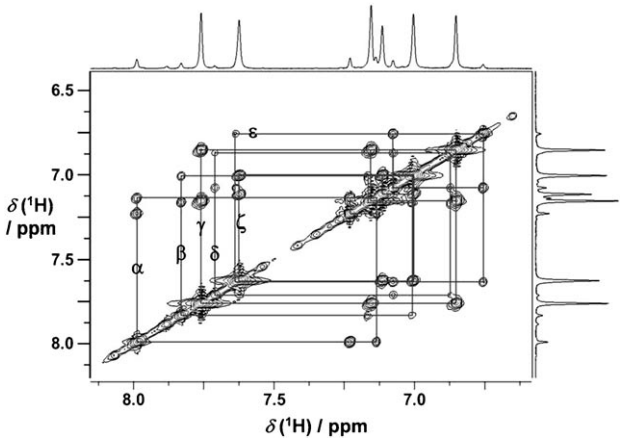

Figure 5. Part of the 2D [^{1}H, ^{1}H] NOESY NMR spectrum of complex $^{15}N_2$-**1** (8.6 mM) in presence of 1-methylimidazole (molar ratio 1:1.02) in 90% PBS/10% D_2O (Ar-saturated, initial pH 8.7) after 2 h of irradiation (λ_{max} = 365 nm, P = 6.4 mW cm^{-2}, dose = 46.1 J cm^{-2}, final pH 10.2) at 310 K. See Table 1 for species assignment.

tains Pt^{II} coordinated to four 1-methylimidazole ligands through N^3. The crystallographic data (space group $P-1$, a = 8.07470(10), b = 9.12370(10), c = 9.3090(2) Å, α = 71.9540(10), β = 65.9410(10), γ = 83.3230(10)°) are in close agreement with the published data. Species α and β can be assigned to *trans*- and *cis*-[Pt^{II}(NH$_3$)$_2$(1-MeIm-N^3)$_2$]$^{2+}$, respectively,[21–23] whereas the minor species δ and ε have not been identified. For comparison purposes, each of the three identified Pt^{II} species (α, β and γ) were synthesised individually, according to literature procedures,[24] and their NMR spectra (Figure S1–S4) compared to the peaks in the spectrum of the irradiated solution. The presence of all three species was confirmed by this method (see Table 1 for chemical shift assignments). Surprisingly, unreacted 1-methylimidazole (ζ) was detected as a major component of the investigated solution, even though the reactants were mixed in a 1:1 molar ratio. The large upfield shift of the ^{15}N^3 resonance (ca. 90 ppm, compared to δ(^{15}N^3) of free 1-methylimidazole at 221.08 ppm) observed for all the new 1-methylimidazole species is consistent with coordination of 1-methylimidazole to platinum taking place through the N^3 atom.[25] The possible coordination of phosphates from the buffer was also ruled out, as in the 1D ^{31}P{^{1}H} NMR spectrum only one peak was detected at 3.84 ppm, arising from the PBS solution itself.

Once the pH of the investigated sample was re-adjusted to 2.6, 1D ^{1}H and 2D [^{1}H, ^{15}N] HSQC NMR experiments were carried out. Based on chemical shifts (Table 2),[14] five peaks as-

Table 1. ^{1}H, ^{13}C and ^{15}N chemical shifts of the peaks produced after 2 h of irradiation (λ_{max} = 365 nm, P = 6.4 mW cm^{-2}, dose = 46.1 J cm^{-2}, 310 K) of complex $^{15}N_2$-**1** (8.6 mM) in presence of 1-methylimidazole (molar ratio 1:1.02) in 90% PBS/10% D_2O (Ar-saturated, pH 8.7 (initial)/10.2 (final)), and of the individually synthesised Pt^{II}-(1-MeIm) complexes (see Figures 4, 5, 6 and Supporting Information).

	Chemical shift [ppm]					
	δ(C***H***$_3$/C***H***$_3$)	δ(C^2***H***/C^{2}H)	δ(C^4***H***/C^{4}H)	δ(C^5***H***/C^{5}H)	δ(***N***^{1})	δ(***N***^{3})
detected species[a]						
α	3.78/35.02	7.99/140.01	7.14/128.94	7.23/123.47	146.42	127.48
β	3.76/34.96	7.83/139.53	7.02/127.57	7.16/122.04	144.86	n.d.
γ	3.73/35.04	7.76/140.08	6.85/128.87	7.15/123.13	146.03	131.09
δ	3.68/34.89	7.71/140.02	6.87/129.56	7.08/122.92	n.d.	n.d.
ε	3.67/34.99	7.64/139.23	6.76/128.32	7.07/122.98	145.35	133.82
ζ	3.72/33.73	7.63/139.40	7.01/128.26	7.12/122.10	141.74	221.08
synthesised complexes[b]						
trans-[Pt^{II}(NH$_3$)$_2$(1-MeIm-N^3)$_2$]$^{2+}$	3.82/35.03	8.05/139.94	7.19/129.00	7.26/123.51	–	–
cis-[Pt^{II}(NH$_3$)$_2$(1-MeIm-N^3)$_2$]$^{2+}$	3.73/34.96	7.78/139.55	7.04/128.55	7.16/123.19	–	–
[Pt(1-MeIm-N^3)$_4$]$^{2+}$	3.73/35.04	7.77/139.93	6.86/128.81	7.16/123.05	–	–

[a] α = *trans*-[Pt^{II}(NH$_3$)$_2$(1-MeIm-N^3)$_2$]$^{2+}$; β = *cis*-[Pt^{II}(NH$_3$)$_2$(1-MeIm-N^3)$_2$]$^{2+}$; γ = [Pt^{II}(1-MeIm-N^3)$_4$]$^{2+}$; δ,ε = unidentified, ζ = free 1-MeIm. [b] In D_2O.

Table 2. ^{1}H and ^{15}N chemical shifts and assignments of the Pt-NH_3 peaks produced after 2 h of irradiation ($\lambda_{max}=365$ nm, $P=6.4$ mW cm^{-2}, dose = 46.1 J cm^{-2}, 310 K) of complex $^{15}N_2$-**1** (8.6 mM) in presence of 1-methylimidazole (molar ratio 1:1.02) in 90% PBS/10% D_2O (Ar-saturated, pH 8.7 (initial)/10.2 (final; re-adjusted to 2.6)). Data obtained from a 2D [^{1}H, ^{15}N] HSQC NMR experiment.

Chemical shifts [ppm] $\delta(^{1}H)$	$\delta(^{15}N)$	Assignment
4.23	−67.00	*trans*-{N-Pt^{II}-$^{15}NH_3$}
4.05	−65.05	*trans*-{N-Pt^{II}-$^{15}NH_3$}
4.04	−65.12	*trans*-{N-Pt^{II}-$^{15}NH_3$}
4.25	−63.45	*trans*-{N-Pt^{II}-$^{15}NH_3$}
4.04	−61.46	*trans*-{N-Pt^{II}-$^{15}NH_3$}
7.12	−1.90	$^{15}NH_4^+$

signable to Pt^{II} species were detected, all consistent with coordinated NH_3 groups *trans* to N-donor ligands. In agreement with results obtained by irradiating complex $^{15}N_2$-**1** on its own under the same experimental conditions, there was no evidence of Pt^{IV}–ammine species, and free $^{15}NH_4^+$ in solution was detected ($\delta(^{1}H/^{15}N)=7.12/-1.90$ ppm), due to the release of ammine ligands upon irradiation.

Discussion

The NMR spectroscopic data obtained during photoactivation of complex **1** allow reaction pathways to be proposed (Scheme 2). According to the literature, in addition to photoredox processes, azido complexes can undergo photosubstitution reactions in which the azido ligand is substituted, for example, by a solvent molecule.[8] This is in agreement with the ^{14}N spectrum of **1** in PBS recorded after only 10 min of irradiation with UVA light (Figure 1b), in which the detected ^{14}N NMR signals are consistent with the presence of Pt^{IV} species of the type *cis*,*trans*,*cis*-[$Pt^{IV}(N_3)(H_2O/OH)(OH)_2(NH_3)_2$] and free N_3^-. Thus, the first step of such photoreactions under these conditions appears to be the release of at least one azido ligand, followed by its replacement with a water molecule, which deprotonates on coordination due to the increase in pH of the solution. However, we cannot rule out the simultaneous and/or subsequent release of, at least, one ammine ligand before reduction of Pt^{IV} to Pt^{II} takes place. A reported study of [$M(N_3)(NH_3)_5$]$^{2+}$, in which M = Cr or Co,[26–28] found that the first photochemical step is the formation of *trans*-[$M(N_3)(H_2O)(NH_3)_4$]$^{2+}$ caused by the photolabilisation of the ammine ligand *trans* to N_3^- due to a strong *trans*-effect of the azido ligand. Thus, depending on the experimental conditions, the generated aqua complexes may undergo subsequent redox (M = Co) or substitution (M = Cr) reactions. Also, it has been reported recently that the photoreduction of some Pt^{IV}–dichlorotetrammine complexes is accompanied by the release of ammonia.[29] In our case, the loss of ammine ligands has been widely confirmed by NMR spectroscopy, thus explaining the formation of insoluble hydroxo-/oxo-bridged polymerised species and the increase of basicity. It is surprising that although photoreduction of the starting Pt^{IV}–diazido complexes in PBS solution occurs, the azido ligands are not oxidised to N_2. This behaviour differs from that observed previously in which irradiation of complex **1** in acidic aqueous solution led to several Pt^{II} species together

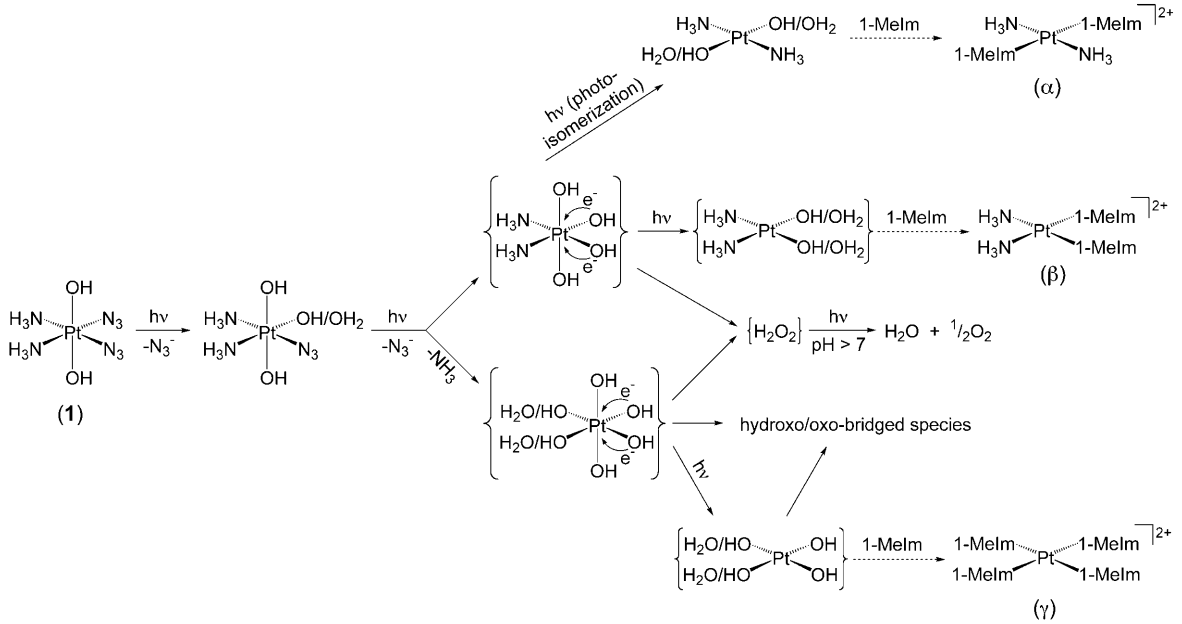

Scheme 2. Possible pathways for photoreactions of complex **1** in PBS. Dashed arrows refer to reactions in presence of 1-methylimidazole, and curly brackets are used to denote transient intermediates. The photodecomposition pathways of **1** in acidic aqueous solution have been reported previously;[30] they involve not only photoreduction to Pt^{II} and O_2 evolution, but N_2 release via nitrene intermediates, in contrast to N_3^- release as detected in the present work.

with the evolution of gaseous dinitrogen by the formation of nitrene intermediates.[30] This emphasises that the observed photoreaction pathways are highly dependent on the solution conditions.

After replacement of both azido ligands, photoreduction may occur by one-electron transfers from each of two hydroxo groups coordinated to the Pt^{IV} centre leading to the corresponding Pt^{II} species together with the formation of hydroxyl radicals. When generated at high local concentrations, hydroxyl radicals readily dimerise to H_2O_2.[31] On irradiation with UV light, hydrogen peroxide is known to decompose by disproportionation to water and gaseous dioxygen (O_2), with a maximum rate at pH 11.6.[32] After each irradiation experiment, the solution was checked for hydrogen peroxide content by means of peroxide test sticks, but no H_2O_2 was detected. However, since in our system pH increases to approximately 10.1 on irradiation, the decomposition of hydrogen peroxide is expected to be favoured. Although the evolution of O_2 was only measured qualitatively, the experimental evidence does support the hypothesis of the involvement of reactive oxygen-containing species (as shown in Scheme 2), which are subsequently oxidised to O_2, while Pt^{IV} complexes are reduced to the corresponding Pt^{II} photoproducts. The detection of O_2 as a photoproduct suggests that a variety of photodecomposition pathways in additions to that shown in Scheme 1 can occur, depending on the actual experimental conditions.

Finally, it is worth noting that on irradiation of complex **1** and its ^{15}N-labelled analogue $^{15}N_2$-**1**, the only detected Pt^{II} photoproduct has NMR parameters consistent with a *trans*-diammine species. This could result from photoisomerisation processes, which lead to the formation of the more thermodynamically stable *trans*-isomer. On absorption of a photon, some complexes may undergo rearrangement of their structure. Photoisomerisation of Pt^{IV}–am(m)ine compounds has been previously observed;[29,33,34] in addition, a number of photoisomerisations of Pt^{II} complexes, including *cis*-$[Pt^{II}(N_3)_2(PPh_3)_2]$ and *cis*-$[PtCl_2(N\text{-amp})_2]$ (*N*-amp = diethyl aminomethylphosphonate), are known to occur from an excited state by a twisting mechanism, that is, without bond-breaking and bond-forming.[35,36] Our experimental evidence does not show whether *cis*-to-*trans* conversion occurs before or after reduction takes place.

It is intriguing that when irradiation studies of complex **1** were carried out in the presence of one molar equivalent of 1-methylimidazole, unreacted 1-methylimidazole was still present in the final solution. If the first step of the investigated photoreaction involves the replacement of the azido ligands with water molecules, then the subsequent photoreduction process would lead to the formation of Pt^{II}–aqua species. Given that in our system the pH increases to 10.2 on irradiation, coordinated H_2O molecules are expected to be readily deprotonated, thus leading to Pt^{II} species in which replacement of hydroxo ligands by free imidazole is unlikely to occur.[18,37] In fact, some of the peaks detected in the 2D [^1H,^{15}N] HSQC NMR spectrum might be assignable to Pt^{II}–hydroxo species containing *trans*-$\{Pt^{II}(NH_3)_2\}$ fragments, thus accounting for the lack of coordination by the free 1-methylimidazole. The fact that a major photoproduct is $[Pt^{II}(1\text{-MeIm-}N^3)_4]^{2+}$, confirms the high affinity of complex **1** toward imidazole rings upon irradiation, and suggests that coordination by 1-methylimidazole and consequent replacement of the NH_3 ligands is favoured as long as the pH of the solution is low enough to give rise to coordinated aqua ligands, which are easily substituted. However, our experimental evidence does not indicate whether coordination of 1-methylimidazole to platinum occurs before or after reduction takes place.

Conclusions

Pt^{IV}–diazido complexes show promise as anticancer agents. They are relatively non-toxic in the dark and can be photoactivated by light to produce new species that are cytotoxic to cancer cells by a novel mechanism of action.[6,7] This may involve the formation of unusual platinated lesions on DNA,[5,38] and initial work has shown that the rapid reactions with guanine derivatives can occur often with seemingly simple pathways in which Pt^{II}–guanine adducts are accompanied by the release of N_2. However, it is also apparent that the reaction pathways that accompany these photoactivated processes are dependent on the solution conditions (e.g., pH, buffer); for example, nitrene intermediates can be trapped in the presence of dimethylsulfide.[30] In the present work, we have shown that photoinduced release of azide from *cis*,*trans*,*cis*-$[Pt^{IV}(N_3)_2(OH)_2(NH_3)_2]$ is facile in phosphate buffered saline solution, and that photoinduced isomerisation can occur.

Our investigation of these reaction pathways has benefited from the use of ^{14}N NMR spectroscopy (99.63% natural abundance, receptivity 1.0×10^{-3} relative to ^1H). There are relatively few reports of the use of this technique in the study of platinum drugs in the literature.[39] The major drawback is ^{14}N quadrupolar relaxation (^{14}N nuclear spin (I) = 1), which dominates when the environment of ^{14}N has a low symmetry and can lead to very broad lines. More commonly, ^{15}N NMR ($I = {}^1/_2$) has been employed in the study of platinum anticancer drugs, despite the low receptivity (3.85×10^{-6} relative to ^1H), as for most compounds of interest ^{15}N-labelled derivatives can be prepared from readily available starting materials.[14,37] A combination of these two NMR techniques has provided us with new insights into the mechanism of photoactivation and photodecomposition pathways.

Our work on photoinduced reactions of *cis*,*trans*,*cis*-$[Pt^{IV}(N_3)_2(OH)_2(NH_3)_2]$ in the presence of 1-methylimidazole suggests that histidyl side chains in proteins could be a target for attack in cells. Intriguingly, under the conditions of our experiments, ammonia release was readily observed together with O_2 production, as well as azide displacement. The formation of the *tetrakis* adduct even at low Pt:1-methylimidazole ratios (1:1) was surprising and illustrates further that photoactivation can lead to unexpected reaction pathways. This is encouraging for the discovery of anticancer

drugs with novel mechanisms of action, drugs which may not be cross-resistant to existing chemical agents.

Experimental Section

Materials: $K_2[Pt^{II}Cl_4]$ was purchased from Precious Metals Online; KI, NaN_3, KOH, and NaCl from Fisher Scientific; $AgNO_3$, NH_4Cl, $^{15}NH_4Cl$, 1-methylimidazole, phosphate buffered saline tablets (1 tablet in 200 mL of water: 0.01 M phosphate pH 7.4, 0.138 M NaCl, 0.0027 M KCl), 1,4-dioxane, and D_2O from Sigma–Aldrich; H_2O_2 (30%) from Polabo; and $HClO_4$ from Fisons.

Warning! Heavy-metal azido complexes are known to be shock-sensitive detonators. We encountered no problems in this study, but these materials should be handled with extreme caution, especially not to put pressure on them in the crystalline form.

Syntheses: Complex *cis*,*trans*,*cis*-$[Pt^{IV}(N_3)_2(OH)_2(NH_3)_2]$ (**1**) and the corresponding ^{15}N-ammine-labelled analogue *cis*,*trans*,*cis*-$[Pt^{IV}(N_3)_2(OH)_2(^{15}NH_3)_2]$ ($^{15}N_2$-**1**) were synthesised as previously described.[16,38] For $^{15}N_2$-**1**, $^{15}NH_4Cl$ was used as the source of ^{15}N. Yield: 78–80%. ^1H NMR (500.1 MHz, 90% H_2O/10% D_2O, pH 5.4, TSP): $\delta = 5.12$ ppm ($^1J(^{15}N,H) = 73$ Hz, $^2J(^{195}Pt,H) = 46$ Hz; Pt^{IV}–$^{15}N\boldsymbol{H}_3$); 2D [^1H, ^{15}N] HSQC NMR (500.1/50.7 MHz, 90% H_2O/10% D_2O, pH 5.4, $^{15}NH_4Cl$): $\delta = -40.8$ ppm ($^1J(^{195}Pt,^{15}N) = 261$ Hz; Pt^{IV}–$^{15}\boldsymbol{N}H_3$); $^{14}N\{^1H\}$ NMR (36.1 MHz, 90% PBS/10% D_2O, pH 7.4, NH_4Cl): $\delta = 353.3$ (Pt^{IV}–NN***N***), 227.4 (Pt^{IV}–N***N***N), 160.5 (Pt^{IV}–***N***NN), −40.8 ppm ($^1J(^{195}Pt,^{14}N) = 180$ Hz; Pt^{IV}–***N***H_3).

Complexes *cis*-$[Pt^{II}(NH_3)_2$(1-MeIm-$N^3)_2]Cl_2$, *trans*-$[Pt^{II}(NH_3)_2$(1-MeIm-$N^3)_2]Cl_2$ and $[Pt^{II}$(1-MeIm-$N^3)_4]Cl_2$ were synthesised according to literature procedures.[24] See Table 1 and Supporting Information for NMR characterisation.

NMR spectroscopy. All NMR spectra were acquired in 90% PBS/10% D_2O (unless otherwise stated) at 298 K on a Bruker DPX300 spectrometer with a QNP [^1H,^{13}C,^{19}F,^{31}P] probe head, a Bruker DPX400 spectrometer with a DUL [^1H,^{13}C] probe-head, a Bruker DMX500 spectrometer with a TBI [^1H,^{13}C,X] probe-head and a Bruker Avance 600 spectrometer with a TXI [^1H, ^{13}C, ^{15}N] cryoprobe-head, all equipped with *z*-field gradients. Data processing was carried out by using XWIN-NMR version 3.5 and MestReC version 4.9.9.9 (Mestrelab Research S.L.).

Typical acquisition parameters for 1D ^1H NMR spectra (^1H: 400.12, 500.13 or 599.92 MHz): 16 transients, spectral width 7.5 kHz, 32k data points and a delay time of 2.0 s. Water suppression was achieved by using a 55.0 dB power-level presaturation. Spectra were processed using exponential weighting with a resolution of 0.5 Hz and a line-broadening threshold of 0.1 Hz.

Typical acquisition parameters for 1D $^{14}N\{^1H\}$ NMR spectra (^{14}N: 36.13 MHz): 64k transients, spectral width 20 kHz, 32k data points and a delay time of 0.25 s. Sequences were optimised for $^1J(^{14}N\text{-}H) = 60$ Hz, and ^1H decoupling was achieved by using WALTZ16 pulse sequence. Spectra were processed using exponential weighting with a resolution of 0.6 Hz and a line-broadening threshold of 10 Hz.

Typical acquisition parameters for 1D $^{13}C\{^1H\}$ PENDANT NMR spectra (^{13}C: 100.60 MHz): 512 transients, spectral width 25 kHz, 64k data points and a delay time of 2 s. Sequences were optimised for $^1J(^{13}C\text{-}H) = 145$ Hz, and ^1H decoupling was achieved by using WALTZ16 pulse sequence. Spectra were processed using exponential weighting with a resolution of 2 Hz, and a line-broadening threshold of 2.8 Hz.

Typical acquisition parameters for 1D $^{31}P\{^1H\}$ NMR spectra (^{31}P: 202.46 MHz): 512 transients, spectral width 20 kHz, 32k data points and a delay time of 1.5 s. ^1H decoupling was achieved by using WALTZ16 pulse sequence. Spectra were processed by using exponential weighting with a resolution of 0.6 Hz and a line-broadening threshold of 10 Hz.

Typical acquisition parameters for 2D [^1H,^1H] NOESY NMR spectra (^1H: 500.13 MHz): 1k transients of 32 scans/block, spectral width 5.0/5.0 kHz, 1k/1k data points and a delay time of 1.5 s. Spectra were processed by using sine weighting with a resolution of 4.8/9.8 Hz and a line-broadening threshold of 0.8/1.5 Hz.

Typical acquisition parameters for 2D [^1H,^{13}C] HSQC NMR spectra (^1H: 500.13/^{13}C: 125.77 MHz): 2k transients of 64 scans/block, spectral width 5.4/17.6 kHz, 2k/2k data points and a delay time of 1.7 s. Sequences were optimised for $^1J(^{13}C\text{-}H) = 145$ Hz, and ^1H decoupling was achieved by using WALTZ16 pulse sequence. Spectra were processed by using cosine-squared weighting with a resolution of 2.7/34.4 Hz and a line-broadening threshold of 0.7/2.5 Hz. ^1H chemical shifts were referenced to TSP by internal 1,4-dioxane at 3.764 ppm.

Typical acquisition parameters for 2D [^1H,^{15}N] HSQC NMR spectra (^1H: 500.13/^{15}N: 50.70 MHz): 512 transients of 16 scans/block, spectral width 7.5/4.6 kHz, 2k/2k data points and a delay time of 1.5 s. Sequences were optimised for $^1J(^{15}N\text{-}H) = 76$ Hz, and ^1H decoupling was achieved by using WALTZ16 pulse sequence. Spectra were processed by using cosine-square weighting with a resolution of 2.2/3.7 Hz and a line-broadening threshold of 0.7/1.0 Hz.

Typical acquisition parameters for 2D [^1H,^{15}N] HMBC NMR spectra ($^1H = 599.92/^{15}N$: 60.79 MHz): 512 transients of 32 scans/block, spectral width 6.0/6.1 kHz, 2k/2k data points and a delay time of 1.5 s. Sequences were optimised for $^1J(^{15}N,H) = 76$ Hz/$^nJ(^{15}N,H) = 6$ Hz, and ^1H decoupling was achieved by using WALTZ16 pulse sequence. Water suppression was achieved by using a 47.0 dB power-level presaturation. Spectra were processed by using cosine-square weighting with a resolution of 2.9/6.2 Hz and a line-broadening threshold of 0.7/1.0 Hz.

^1H chemical shifts were referenced to TSP (sodium 3-(trimethylsilyl)-[2,2,3,3-D_4]-proprionate) through internal 1,4-dioxane at 3.764 ppm, ^{13}C to TMS (tetramethylsilane) through internal 1,4-dioxane at 67.19 ppm, ^{14}N and ^{15}N to external $^{15}NH_4Cl$ 1.5 M in 1 M HCl at 0.00 ppm and ^{31}P to external H_3PO_4 85% in D_2O at 0.00 ppm.

pH measurement: pH values were measured at ambient temperature directly in the NMR tube with a Corning 145 pH-meter equipped with an Aldrich microcombination electrode, calibrated with standard Aldrich buffer solutions at pH 4, 7 and 10.

pK_a determination: The experimental pH titration data were fitted to the following formula derived from the Henderson–Hasselbalch equation [Eq. (1)] in which K_a is the dissociation constant for species 1-MeImH$^+$, δ_A, and δ_B are the limiting chemical shifts of species 1-MeImH$^+$ and 1-MeIm, respectively.

$$\delta = \frac{\delta_A \cdot 10^{-pH} + \delta_B \cdot 10^{-pK_a}}{10^{-pH} + 10^{-pK_a}} \quad (1)$$

The pH titration curves (^{14}N chemical shifts of both N^1 and N^3 vs. pH) were fitted using the program ORIGIN version 6.0 (Microcal Software Ltd.).

Photoreactions: Samples for the photochemical studies were 8–15 mM solutions of the investigated Pt^{IV} complexes (on their own or containing 1-methylimidazole in 1:1 molar ratio) in 0.6 mL 90% PBS/10% D_2O. Before irradiation, the samples were transferred into 5 mm screw-cap NMR tubes (Wilmad) provided with a teflon/silicone septum, and Ar-saturated for 30 min. NMR samples were then irradiated for 2 h (unless otherwise stated) at 310 K by using a LZC-ICH2 photoreactor (Luzchem Research Inc.) equipped with a temperature controller and 16 LZC-UVA lamps (Hitachi, $\lambda_{max} = 365$ nm) or 16 LZC-VIS UV-Visible light lamps (Sylvania cool white, $\lambda = 250$–700 nm) with no other sources of light filtration. The spectral outputs for both sources are shown in the Supporting Information (Figure S5). The power levels ($P = 6.4$–7.2 mW cm^{-2} (UVA), $P = 30.0$ mW cm^{-2} (UV/Vis)) were monitored and assessed using the appropriate probe window, calibrated against an OAI-306 UV power meter from Optical Associates, Inc.; the delivered radiation dose (J cm^{-2}) is defined as irradiance (P, W cm^{-2}) × time (s). NMR spectra were then recorded soon after irradiation.

Po_2 measurement: Po_2 values were measured with a Corning 240 pH-meter (switched to read millivolts) equipped with a Lazar DO-166-NP dissolved oxygen needle probe. Calibration was carried out at 295 K and a barometric pressure of 761 mmHg by using a 0.1 g L^{-1} NaCl solution in

double-distilled water (made freshly) giving at equilibrium with atmospheric dioxygen a Po_2 value of 161 mmHg (theoretical: 163 mmHg). The electrode was then set up to read Po_2 directly in mm of Hg partial pressure.

Acknowledgements

We thank the EPSRC, the University of Warwick (studentship for H.I.A.P), the EC (Marie Curie Fellowship for L.R.) and Scottish Enterprise for financial support, Prof. Simon Parsons and Dr. Stephen Moggach for determination of the crystal structure of $[Pt(1\text{-}MeIm)_4](ClO_4)_2$, Mr. Juraj Bella for assistance with NMR experiments, and members of EC COST D39 for stimulating discussions. We are grateful to Warwick-Design for the design of the Frontispiece.

[1] A. Vogler, A. Kern, B. Z. Fusseder, *Naturforsch. B* **1978**, *33*, 1352–1356.
[2] A. Vogler, J. Hlavatsch, *Angew. Chem.* **1983**, *95*, 153–153; *Angew. Chem. Int. Ed. Engl.* **1983**, *22*, 154–155.
[3] P. J. Bednarski, F. S. Mackay, P. J. Sadler, *Anti-Cancer Agents Med. Chem.* **2007**, *7*, 75–93.
[4] L. Ronconi, P. J. Sadler, *Coord. Chem. Rev.* **2007**, *251*, 1633–1648.
[5] J. Kašpárková, F. S. Mackay, V. Brabec, P. J. Sadler, *J. Biol. Inorg. Chem.* **2003**, *8*, 741–745.
[6] P. J. Bednarski, R. Grünert, M. Zielzki, A. Wellner, F. S. Mackay, P. J. Sadler, *Chem. Biol.* **2006**, *13*, 61–67.
[7] F. S. Mackay, J. A. Woods, P. Heringová, J. Kašpárková, A. M. Pizarro, S. A. Moggach, S. Parsons, V. Brabec, P. J. Sadler, *Proc. Natl. Acad. Sci. USA* **2007**, *104*, 20743–20748.
[8] J. Šima, *Coord. Chem. Rev.* **2006**, *250*, 2325–2334.
[9] R. J. Sundberg, R. B. Martin, *Chem. Rev.* **1974**, *74*, 471–517.
[10] W. W. Bachovchin, J. D. Roberts, *J. Am. Chem. Soc.* **1978**, *100*, 8041–8047.
[11] R. B. Martin in *Cisplatin: Chemistry and Biochemistry of a Leading Anticancer Drug* (Ed.: B. Lippert), Wiley-VCH, Weinheim, **1999**, pp. 183–206.
[12] A. Eastman in *Cisplatin: Chemistry and Biochemistry of a Leading Anticancer Drug* (Ed.: B. Lippert), Wiley-VCH, Weinheim, **1999**, pp. 111–134.
[13] L. A. Zwelling, S. Michaels, H. Schwartz, P. P. Dobson, K. W. Kohn, *Cancer Res.* **1981**, *41*, 640–649.
[14] S. J. Berners-Price, L. Ronconi, P. J. Sadler, *Prog. Nucl. Magn. Reson. Spectrosc.* **2006**, *49*, 65–98.
[15] J. E. Kent, E. L. Wagner, *J. Chem. Phys.* **1966**, *44*, 3530–3534.
[16] F. S. Mackay, J. A. Woods, H. Moseley, J. Ferguson, A. Dawson, S. Parsons, P. J. Sadler, *Chem. Eur. J.* **2006**, *12*, 3155–3161.
[17] S. J. Berners-Price, U. Frey, J. D. Ranford, P. J. Sadler, *J. Am. Chem. Soc.* **1993**, *115*, 8649–8659.
[18] T. G. Appleton, A. J. Bailey, K. J. Barnham, J. R. Hall, *Inorg. Chem.* **1992**, *31*, 3077–3082.
[19] M. Alei, Jr., L. O. Morgan, W. E. Wageman, T. W. Whaley, *J. Am. Chem. Soc.* **1980**, *102*, 2881–2887.
[20] O. Clement, A. W. Roszak, E. Buncel, *J. Am. Chem. Soc.* **1996**, *118*, 612–620.
[21] G. V. Fazakerley, K. R. Koch, *Inorg. Chim. Acta* **1979**, *36*, 13–25.
[22] M. M. Muir, M. E. Cadiz, A. Baez, *Inorg. Chim. Acta* **1988**, *151*, 209–213.
[23] D. Gibson, G. M. Arvanitis, H. M. Berman, *Inorg. Chim. Acta* **1994**, *218*, 11–19.
[24] C. G. van Kralingen, J. Reedijk, *Inorg. Chim. Acta* **1978**, *30*, 171–177.
[25] M. Alei, Jr., P. J. Vergamini, W. E. Wageman, *J. Am. Chem. Soc.* **1979**, *101*, 5415–5417.
[26] O. Horvath, K. L. Stevenson, *Charge Transfer Photochemistry of Coordination Compounds*, VCH, Weinheim, **1992**.
[27] V. Balzani, V. Carassiti, *Photochemistry of Coordination Compounds*, Academic Press, New York, **1970**.
[28] H. Hennig, D. Walther, P. Thomas, *Z. Chem.* **1983**, *23*, 446–446.
[29] Y. Nakabayashi, A. Erxleben, U. Létinois, G. Pratviel, B. Meunier, L. Holland, B. Lippert, *Chem. Eur. J.* **2007**, *13*, 3980–3988.
[30] L. Ronconi, P. J. Sadler, *Chem. Commun.* **2008**, 235–237.
[31] O. Legrini, E. Oliveros, A. M. Braun, *Chem. Rev.* **1993**, *93*, 671–698.
[32] K. Azrague, E. Bonnefille, V. Pradines, V. Pimienta, E. Oliveros, M.-T. Maurette, F. Benoit-Marquie, *Photochem. Photobiol. Sci.* **2005**, *4*, 406–408.
[33] R. Kuroda, S. Neidle, I. M. Ismail, P. J. Sadler, *Inorg. Chem.* **1983**, *22*, 3620–3624.
[34] C. F. J. Barnard, J. F. Vollano, P. A. Chaloner, *Inorg. Chem.* **1996**, *35*, 3280–3284.
[35] J. Sýkora, J. Šima, *Coord. Chem. Rev.* **1990**, *107*, 1–212.
[36] D. Cornacchia, L. Cerasino, C. Pacifico, G. Natile, *Eur. J. Inorg. Chem.* **2008**, 1822–1829.
[37] J. Vinje, E. Sletten, *Anti-Cancer Agents Med. Chem.* **2007**, *7*, 35–54.
[38] P. Müller, B. Schröder, J. A. Parkinson, N. A. Kratochwil, R. A. Coxall, A. Parkin, S. Parsons, P. J. Sadler, *Angew. Chem.* **2003**, *115*, 349–353; *Angew. Chem. Int. Ed.* **2003**, *42*, 335–339.
[39] R. E. Norman, P. J. Sadler, *Inorg. Chem.* **1988**, *27*, 3583–3587.

Received: October 24, 2008
Published online: January 12, 2009

